A TWO-SPOT ALBEDO MODEL FOR THE SURFACE OF PLUTO

ROBERT LOUIS MARCIALIS[a)]
Arthur J. Dyer Observatory, Vanderbilt University, Nashville, Tennessee 37212
Received 21 September 1987; revised 4 November 1987

ABSTRACT

This paper summarizes the work of Marcialis (1983, 1984). A finite-element approach has been used to generate synthetic light curves of an unevenly bright, rotating sphere. Application to the Pluto–Charon system shows that two circular spots (46° and 28° in radius, both at south latitude 23°, separated by 134° in longitude) with albedos half that of the surrounding terrain can accurately reproduce six available photoelectric light curves between 1953 and 1982. A dark equatorial band (extending from south latitude 69° to anywhere between 50° and 65° north latitude) can be invoked to explain the secular dimming. Constraints on this equatorial band, which may alternatively be viewed as two polar caps, are such that to date its dimensions are not uniquely determined. However, polar caps with albedos near unity serve quite well to explain the 40% dimming of Pluto since its discovery in 1930. Hardie's 1964 photoelectric observations are presented for the first time in tabular form.

I. INTRODUCTION

Successful analysis of light curves for two classes of variable stars using spot models has been in progress for about a decade and a half (cf. Torres and Ferraz-Mello 1973; Vogt 1975, 1980; Eaton and Hall 1979; Poe 1983). These models call for isolated regions of relatively cooler (and therefore darker) photosphere to explain the amplitude and phase characteristics of photometric data. Presented here is the first application of such techniques to a planetary problem.

Most planetary albedo features may be considered invariant over all but geologic timescales. The orientation of a body's rotational axis can be determined through photometric astrometry (Taylor 1979), and changes in viewing geometry permit observations to be made from differing aspects. This extra information allows ready discrimination between solutions which, in the stellar case, must remain ambiguous.

Both previous attempts to describe the surface-albedo distribution of Pluto (Renschen 1977; Lacis and Fix 1972) were attempts to solve the inverse problem, that is, to postulate the photometric data and work backward to the surface-albedo distribution and scattering properties. The general solution to this problem was treated in detail by Russell (1906). A consequence of this method of attack is heavy reliance upon Fourier analysis to describe the data. In the case of a faint object like Pluto, the paucity of data points and their poor signal-to-noise ratio severely constrains the utility of the Russell method.

Such difficulties are circumvented by the direct technique of spot modeling, which attempts to reproduce the observational data. The price to be paid is that a much larger parameter space must be explored for solutions. In the simplest case, which assumes the spots are at the same latitude, circular, and two in number, the basis of the parameter space is in fact four dimensional. Two radii, a central latitude, and a difference in longitude (hereafter referred to as $R1$, $R2$, ALAT, and DLON, respectively) need to be specified for any given model.

Another penalty of the direct (numerical) approach is that, should a solution be found, there is no guarantee that it is the *only* solution. One first attempts to locate all regions in parameter space (valleys) that possess relatively small residuals. That valley which minimizes residuals under the stated assumptions is adopted as the working solution.

II. THE MODEL

Synthetic light curves were generated by using a finite-element method. The surface of a sphere is divided by a fine grid of longitude and latitude. Each element consists of a small trapezoid, typically 2° or 4° on a side. Bases are bounded by parallels of latitude, and the remaining sides by meridians of longitude. The instantaneous brightness of the planet is obtained by numerically integrating the contributions of all elements in view at a given time. As depicted in Fig. 1, each element is represented by the product of two quantities: the unit vector of its center and its area. The reflectivity of an element is accounted for by multiplying its area by a proportionality constant between zero and unity. By definition, this constant is the geometric albedo (Allen 1973).

Projection effects are accounted for by forming the dot product of the unit vector of each element with that unit vector representing the instantaneous line of sight to the Earth, an operation mathematically equivalent to multiplication by the cosine of the enclosed angle. In many treatments the degree of limb darkening is proportional to some power of this dot product as well. For example, the limb darkening of a Lambertian surface is linear in the dot product.

Other steps are taken to reduce the number of machine operations by several orders of magnitude. These are described below.

Rather than keep track of all elements, only spotted ones (by definition, those in the minority) are considered. To do this, we reference all magnitudes to those of a sphere of uniform (majority) albedo. Thus, the diminution of reflected light caused by visible spotted area is the only time-varying quantity. As shown in the Appendix, a useful side effect of this procedure is that the absolute geometric albedos are lost in favor of the quantity ALBFAC, where

$$\text{ALBFAC} \equiv 1 - \frac{\text{spotted albedo}}{\text{unspotted albedo}}. \quad (1)$$

Implementation of this convenience makes all results independent of the absolute radius of Pluto. Considerable uncertainty existed in our knowledge of Pluto's radius at the time of this study. Using this formulation, Pluto's absolute magnitude and radius are the only quantities required to extract

[a)] Current address: Lunar and Planetary Laboratory, University of Arizona, Tucson, AZ 85721.

 0004-6256/88/030941-07$00.90

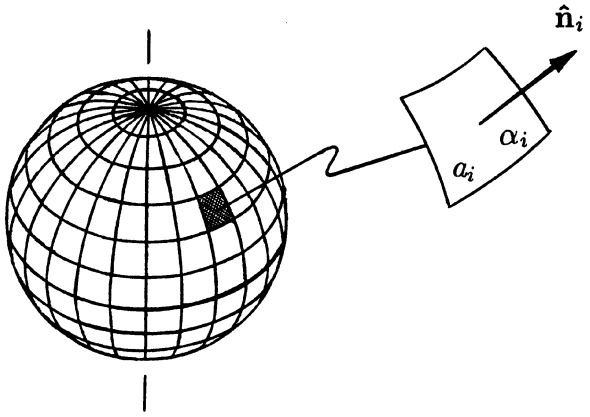

FIG. 1. Finite-element approximation to a sphere. Each ith element is bounded by lines of constant latitude and longitude, has area a_i, normal vector $\hat{n}$, and albedo α_i. The unit vector toward Earth is the normal out of the page. Instantaneous brightness is given by summing the contributions of all elements, after accounting for projection and limb darkening individually. The pictured grid size is 15°; actual calculations were done with 2° or 4° meshes.

a posteriori absolute albedos for any given model.

Further computational advantage is obtained by working in a Plutocentric coordinate system. Spinning the Earthward vector about the planet allows the thousands of unit vectors to remain untouched after their initial calculation. Recalculation of the Earthward vector at each rotational phase neatly avoids the cumulative effects of roundoff error.

The equation for the dimming Δm (in magnitudes) at any specific geometry is derived in the Appendix and is given by

$$\Delta m = -2.5 \log (\text{BRITE}),$$

where (2)

$$\text{BRITE} = 1 - \frac{A_s \times \text{ALBFAC}}{A_E (1+f)},$$

where the areas A are appropriately weighted for projection effects and limb darkening. The quantity f represents the fraction of light contributed by Charon, measured in terms of the light of an "unspotted" Pluto. A value of 0.20 was assumed for f. This has since been shown to be reasonable by Marcialis *et al.* (1987). Experimental verification that the large spot resides on Pluto was obtained by these same authors: the out-of-eclipse light-curve slope persisted even when Charon was totally obscured by Pluto.

III. OTHER ASSUMPTIONS

Pluto's pole position was first determined by Andersson and Fix (1973). The discovery of Charon has allowed this value to be refined, while resolving a $\pm 180°$ ambiguity in the previous determination. Harrington and Christy (1981) give the following equations for Pluto's instantaneous inclination, which were adopted outright:

$$j_0 = 106°,$$
$$j = j_0 - 2.^\circ 2T - 0.^\circ 005T^2, \quad (3)$$
$$i = j + 1.^\circ 8 \cos [2\pi(t - 0.6)],$$

where j is the heliocentric inclination, i is the apparent geocentric inclination, T is the epoch measured from 1980.0, and t is the fractional year. Note that these relations imply that we have been viewing primarily the *southern* hemisphere of Pluto since its discovery in 1930. We define north as *the direction of the angular momentum vector of the planet*. Although this is not the IAU definition of north (Davies *et al.* 1980), it is both a simpler and less ambiguous convention to use.

A phase coefficient of 0.031 mag/degree (Tholen and Tedesco 1983) was assumed. Since this work was completed, Binzel and Mulholland (1983) have computed a value of 0.041 ± 0.003 mag/deg. As Pluto never deviates more than $\sim 1.^\circ 8$ from the antisolar direction, any error introduced by adopting the lower value is small (and systematic, as most of the published light curves were obtained over short intervals). Reduction of all observations to 1° serves to minimize potential complications due to the opposition effect.

The literature contains several *ad hoc* assumptions of extreme limb darkening on Pluto, none of which have proven to be necessary. A moderate linear limb-darkening coefficient of 0.5 was adopted in order to split the range of possible values. Once an acceptable solution was obtained, the problem was reworked using $x = 0.0$ and $x = 1.0$. While possible to find solutions with absolutely no limb darkening, the best solution with $x = 1$ was clearly unable to reproduce the amplitude behavior of Pluto's light curve.

Two final assumptions are that albedo features have been *static* over the past 30 yr, and that the spots are *darker* than the surrounding terrain. To have overall dimming, either light regions must recede from view or dark regions must approach the sub-Earth point. The former case demands that light spots become progressively more foreshortened over the three decades of observation. Thus the spots contribute less and less to the rotational light curve and amplitudes should decrease, exactly the opposite of what is observed.

IV. OBSERVATIONS

Photoelectric observations of Pluto were obtained in 1953–1955 (Walker and Hardie 1955), 1964 (Hardie 1965), 1966 (Kiladze 1967), 1971–1973 (Andersson and Fix 1973; Neff, Lane, and Fix 1974), 1975 (Lane, Neff, Andersson, and Fix 1976), 1980–1981 (Tedesco and Tholen 1980; Tholen and Tedesco 1983), and 1982 (Binzel and Mulholland 1982). For brevity, these light curves henceforth will be referred to by their central or median epoch. All have been reduced to a common viewing geometry, that of mean opposition: heliocentric distance 39.5 AU, geocentric distance 38.5 AU, and solar phase angle 1°. A photometric period of $6^d.3867$ (Hardie 1965) and epoch of 2,444,240.661 (Binzel *et al.* 1985) is assumed throughout. A color index $(B - V) = +0.80$ mag is assumed when data obtained after 1980 must be compared with the older data, as in the explanation of the secular dimming.

The 1954 light curve of Pluto is actually a composite obtained over three successive apparitions. Six points obtained by Kuiper in 1953 are systematically fainter than the rest; an arbitrary correction of -0.05 mag was applied to them by Walker and Hardie (1955). Kuiper's points have been excluded from this analysis.

In 1964, Hardie obtained a light curve using the 24 in. Seyfert reflector of the A. J. Dyer Observatory (see Table I). These data were presented at a meeting of the AAS (Hardie 1965), and appeared as a graph in the March 1965 issue of Sky and Telescope with 15 points. Records at the Dyer Observatory show only 14 points comprising this data set. All efforts to verify the authenticity of the datum at approximately 0.6 rotational phase and magnitude $V_0 = 15.0$ have

TABLE I. Photoelectric photometry of Pluto in 1964.

Julian Date	V_0	P.E.	α (deg)
2,438,000 +			
530.750	15.12	0.005	1.692
531.708	15.06	0.005	1.670
532.696	14.99	0.004	1.708
537.633	15.11	0.005	1.740
541.609	14.94	0.004	1.758
545.675	15.01	0.017	1.769
548.722	14.95	0.004	1.772
550.614	15.09	0.005	1.772
551.727	15.05	0.012	1.771
552.617	14.99	0.008	1.769
553.628	14.96	0.006	1.768
554.642	14.96	0.003	1.765
555.644	15.01	0.006	1.763
556.606	15.09	0.009	1.759

proven futile; the existence of this point must be regarded as spurious.

Five points were obtained by Kiladze (1967) in 1966. Alone they are insufficient to define a light curve clearly. Since they are substantially brighter than the 1964 data, they have been excluded from the present analysis.

V. BOUNDS TO MODEL PARAMETERS

Simple geometrical considerations may be invoked which greatly reduce the volume of parameter space in which potential solutions might lie. Consider a circular spot on a unit sphere whose center is coincident with the sub-Earth point. For the sake of simplicity, assume the spot to have zero albedo and the surrounding regions albedo unity. In order to produce the amplitude of $\sim$0.3 mag observed in the later light curves, by necessity the large spot must have a radius of 29°.4. In general, a lower bound to the spot radius $\Theta_{\min}$ may be set by using the relation

$$\Delta m = -2.5 \log \left[1 - \frac{\mathrm{ALBFAC} \sin^2 \Theta_{\min}}{1+f} \right], \qquad (4)$$

which is a consequence of the derivation comprising the Appendix.

Any *lower* limit deduced for the large spot radius serves as the *upper* limit for the small spot radius by definition.

The difference in longitude between spot centers (DLON) may be trivially bounded from above by 180°. An approximate lower bound may be set at $\sim$120°, since separations less than this result in synthetic light curves which are virtually sinusoidal, regardless of the contrast ratio chosen.

Both upper and lower bounds may be determined for the mean contrast ratio or, equivalently, ALBFAC. By its definition, ALBFAC must necessarily lie between zero and unity. The lower extremum may be further raised through a slightly different application of Eq. (4). If a maximum spot radius of 90° is assumed, we find that ALBFAC for the two hemispheres must be greater than 0.24 to produce the maximum observed photometric amplitude. Taking Charon's contribution f to be 20% raises the limit to 0.29. Thus ALBFAC has been constrained to lie between 1.00 and 0.29, i.e., the albedo ratio of spotted to unspotted regions must lie between 0.00 and 0.76. In the subsequent analysis, we demand the contrast ratio to be constrained at 1:2.

Finally, the central latitude of the spots may be somewhat constrained. The amplitude of Pluto's light curve has been monotonically increasing over the past 30 yr. The sub-Earth point is approaching the equator from the south. These two facts make it plausible to believe that the spots are not yet being seen "face on". According to Eq. (3), the sub-Earth point during the 1980 apparition was at 16° south latitude. Admitting that Pluto's spots may deviate significantly from exact circularity, we can adopt $-20°$ as an approximate southernmost limit to ALAT, the central latitude.

VI. METHOD OF SOLUTION

Any given light curve may be satisfactorily described by three quantities: an amplitude, a reference brightness, and an "asymmetry parameter," all of which are changing functions of time. In the past, the maximum, minimum, or mean brightness has been used as a reference. A more meaningful quantity in the context of this work is the theoretical "unspotted brightness," namely, the brightness Pluto would have if it were a uniform sphere of albedo equal to that of the unspotted regions. An asymmetry parameter is harder to quantify. The ratio of "rise time" to "fall time" for a given light curve, while insufficient to describe the detailed structure, is nevertheless very useful.

To systematize the search for an acceptable solution, it was assumed that these three light curve characteristics are to first order separable. Trends noticed during the developmental stage of the model have shown this to be a reasonable assumption. It was decided first to attempt to match the increasing amplitude behavior of the light curves while ignoring shape and secular dimming. The use of contour plots in parameter space was found to be an expedient method of search.

First, the amplitude of each light curve was estimated visually. Next, the radius of the larger spot (R 1) and a difference in longitude were fixed. The remaining two parameters, R 2 and ALAT, were then allowed to vary, by 5° or 2.5° increments. For each combination of these latter two parameters, a synthetic light curve was generated and the amplitude for each epoch noted. Residuals in amplitude were calculated, and the sum of their absolute values plotted in the R 2–ALAT plane. Isoresidual points were connected with smooth curves to give a contour plot. This process was repeated for 5° increments of both big spot radius and differential longitude. The minimum of each contour plot was then selected. These minima delineated the approximate boundaries of the subset of amplitude-matching parameter combinations, plus or minus about 5° in any parameter. With the amplitude-matched subset thus determined, consideration of asymmetry and detailed light curve structure was examined next.

Inspection showed that, for a given latitude, the requisite spot radii are nearly independent of the longitude separating the two spots. However, asymmetry *does* appear to be a strong function of differential longitude. If spot centers are closer in longitude than $\sim$120°, there is very little asymmetry; the resulting light curve appears virtually sinusoidal. Well before the extremum of 180° separation is reached, usually around 150° to 160° separation, the synthetic light curves break up into double-humped functions for the latter (nearly equator-on) epochs. It was a fairly straightforward matter to sift through the amplitude-matched subset of candidates to determine which of these also met the appropriate asymmetry and shape criteria.

A visually satisfying fit to the data having thus been achieved, a method of differential corrections was developed to determine the best solution. One approach to measuring the goodness of fit is through the chi-squared statistic (Bev-

ington 1969). Chi-squared (χ^2) is the sum over all observations of the square of the observed minus the calculated value, divided by the square of the error estimate for each observation.

Instantaneous inclination and rotational phase were determined for the Julian Date of each datum. Corresponding values of Δm for an entire data set were calculated. A routine was implemented to determine the additive zero-point shifts in both abscissa and ordinate necessary to best align the real and synthetic data. The offset along the ordinate corresponds to the best reference (i.e., unspotted) brightness for a particular set of model parameters. The shift along the time axis is a somewhat more complicated parameter. It is comprised of the sum of corrections to location of the large spot center (which initially had been assumed to lie at 0° longitude exactly), small errors in the assumed value for photometric period, epoch, light-time delay between Pluto and Earth, and deviations of the large spot from circularity. The two additive constants were determined to 0^m001 and 0^d001, respectively.

All four model parameters were incremented in steps of 1°, and χ^2 calculated. The best solution to each light curve was taken as that set of parameters and shifts that minimized χ^2. This procedure was repeated independently for all data sets; as a consistency check, the 1980 and 1981 data were treated independently. Results appear in Table II. Note the tight cluster in three of the four free parameters for all epochs considered. The small deviations are remarkable in light of the simplifying assumptions made, particularly that of strictly circular spots. The lone exception is the apparent bimodal clustering of the differential longitude. However, note that the size of the disagreement is only half the diameter of the smaller spot. An elongated or elliptical secondary spot could easily account for most of the disagreement, should the long axis be aligned southwest to northeast. The signal-to-noise ratio of the photometry is probably insufficient to warrant a detailed examination of this possibility. Because of the similarity of "best-fit" solutions for all epochs, the adoption of a single set of parameters may be justified.

Comparison of the temporal behavior of models having "wide" and "narrow" differential longitudes is a useful exercise. The 1954-optimized parameters produce light curves that evolve to double-humped functions for later years, since at nearly equator-on viewing geometry the two spots are viewed essentially independent of one another. As early as 1972, the match with real data is quite unsatisfactory. Conversely, when the 1980-optimized model is compared to the early data there is much less disagreement. Synthetic data for the middle portion of the 1954 light curve is too bright by about 2%; disagreement with the 1964 data is even less. For these reasons, the parameters labeled "adopted" at the foot of Table II have been assumed for our provisional working model. Fits to all subsets of data have been made, and appear as Fig. 2.

TABLE II. Optimum fits to each data set.

Year	$R1$	$R2$	LAT	DLON	UNSPOT[a]	N	χ^2
1954.2	46	28	−23	−161	14.740	21	184.6
1964.4	44	28	−20	−162	14.858	14	75.4
1972.4	46	27	−22	−134	14.988	46	38.1
1975.2	46	25	−29	−131	14.946	12	3.08
1980.2	47	26	−24	−133	15.844	24	50.2
1981.2	45	28	−22	−132	15.842	18	181.7
1982.2	46	29	−7	−133	15.854	31	83.4
Adopted:	46	28	−23	−134			

[a] Pluto's magnitude should spots be removed. $V_0(1°)$ before 1980, $B_0(1°)$ after 1980.

A potential zero-point error in the 1955 observations has been previously noted (Hardie, personal communication; Andersson and Fix 1973). Using the provisional model, we find that a correction of +0.024 mag to these data lowers the value of χ^2 to only 58% of its uncorrected value as reported in Table II.

VII. THE SECULAR DIMMING

Having arrived at a satisfactory explanation for the amplitude and shape behavior of Pluto's light curve, a search for a geometrical explanation of the secular dimming was undertaken. This dimming may alternately be called the "orbital light curve". In order to have overall dimming, either light regions must recede from view, or dark regions must approach the sub-Earth point as the apparent inclination changes with time. Should the cause of this secular dimming have longitudinal dependence, synthetic light-curve amplitudes and shapes would necessarily be altered by the addition of further light or dark regions. This also violates our assumption of separability of light-curve characteristics. Therefore, the simplest geometric explanation should have latitudinal symmetry; e.g., circumpolar bands or caps.

Such "band" models are computationally efficient. Since there is no longitudinal dependence, only one numerical integration per central epoch is required. Moreover, the results of two-spot and band models are additive, given that there is no overlap to the albedo features. The same reference magnitude is defined for each epoch as before, that corresponding to the integrated brightness of a uniform sphere with all markings (spots and bands) removed; e.g., with the albedo of the polar regions.

The problem now reduces to one of finding a band geometry that reproduces the theoretical unspotted brightness behavior for all central epochs of photometric data (column 6 of Table II). A geometric solution is considered satisfactory only if a uniform-albedo brightness can be found that is constant for all years should the band be removed.

Circumpolar-band models were generated at 5° increments of width and central latitude. All allowable combinations, from the maximum of global coverage (an equatorially centered band 180° thick) to the minimum of a vanishingly narrow stripe were examined. Northern and southern boundaries were varied separately. The general trend of the orbital light curve can be matched by a whole suite of band models (a long, shallow "valley" in parameter space). Goodness of fit does not seem to be very sensitive to choice of either contrast ratio or degree of limb darkening. A means of evaluating the relative merit of these acceptable solutions had to be found.

Photographic and visual photometry was carried out during the post-discovery years of the early 1930s. These observations are well summarized by Andersson (1974). Although the quality of these observations is poor compared to modern photoelectric photometry, they nevertheless cluster between $V_0 = 14.6$ and $V_0 = 14.8$. The handicap of this large uncertainty is offset partially by the fact that these early observations serve to double the time base provided by the photoelectric observations alone. Extrapolation of candidate models back to the 1930s *does* serve to constrain further the

set of acceptable solutions, but to use the photographic estimates as a discriminant between which models are and are not acceptable would be extremely irresponsible.

As opposed to the two dark equatorial spots, *extreme* uniqueness problems exist in the determination of a third albedo feature that explains the orbital light curve of Pluto. Most acceptable band models have in common latitudinal widths of more than about 110°; values of ALBFAC between 0.8 and 1.0 (i.e., a contrast ratio of 5:1 or greater) seem to be required as well. In this sense, it is equivalent to think of Pluto as having two very bright (albedos approaching unity) polar caps. To maintain such high-albedo material, global transport of volatiles must occur on a ≪ geologic timescale, perhaps as short as the Plutonian year. In this case, to assume polar caps of fixed dimensions may be unrealistic.

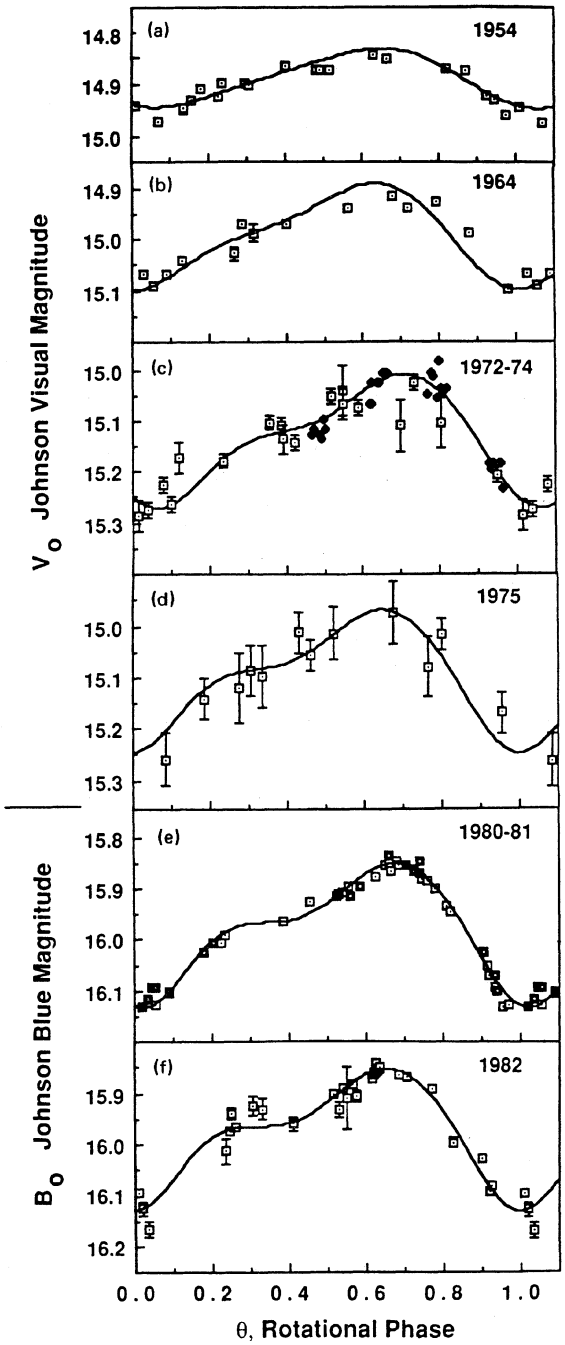

FIG. 2. (a–f) Theoretical fit to photometric data using the adopted model parameters. Ordinate is visual magnitude at mean opposition and 1° solar phase angle.

The southern cap, which has been in sunlight since before Pluto was discovered, is smaller than the northern (winter) cap and abuts the large spot for *all* suitable models, regardless of albedo ratio or limb-darkening coefficient chosen. Conversely, the extent of the north polar cap is very poorly constrained. All that can be said at this time is that its boundary probably lies between 50° and 65° north latitude. The reason for its indeterminacy is rather simple. Due to the orientation of Pluto's pole, the boreal polar regions were not seen at least until Andersson's 1972 photoelectric measurements. Therefore, only one-third to one-half the observational time base exists as for the dark, equatorial spots. Any claim to have discerned its exact dimensions must be regarded lightly.

Figure 3 shows the behavior of one of the better band-model candidates. The parameters for this model are as follows: center at − 5° latitude, width 128°, ALBFAC 0.9, and linear limb-darkening coefficient 0.5. Most poorly constrained of these parameters is the northern boundary. The mean residual per light curve is 0.02 mag. This is comparable to the mean probable error in absolute flux calibration for the comparison star of each epoch. Many other solutions exist with similar residuals; this particular solution is adopted only for the sake of concreteness. Should the polar caps be nonstatic in nature, then their degree of indeterminacy would increase still further. Consideration of such more complicated models would be beyond both the scope of this work and the precision of the data.

VIII. RESULTS

A crude albedo map for the surface of Pluto emerges as the primary result of this study. Depicted in Fig. 4, these results can serve as a "working template" against which observations of the ongoing mutual events between Pluto and Charon may be compared. Subtraction of any anticipated out-of-eclipse photometric variability is a necessary first step in interpreting such mutual-event observations for accurate values of radii, albedos, and oblatenesses through either

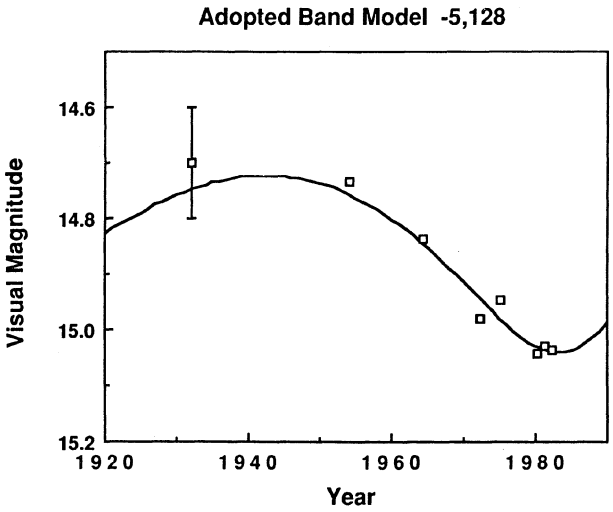

FIG. 3. Photometric behavior of adopted band model. Provisional model parameters are denoted above the panel. Due to the large uncertainty in the 1934 photographic point, it is difficult to constrain rigorously the sizes and relative albedos of polar caps and the darker equatorial region.

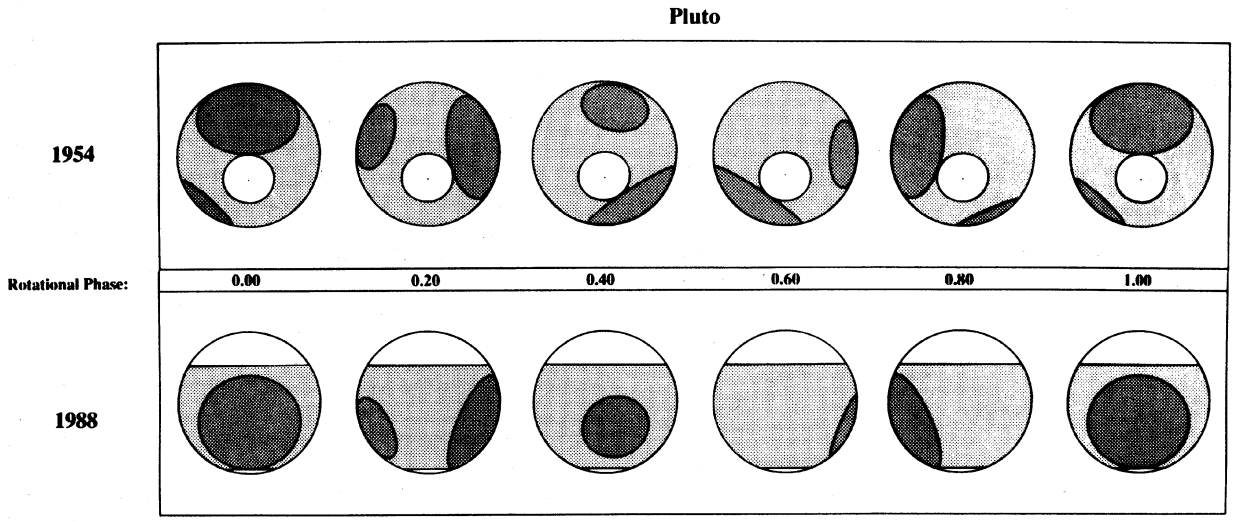

FIG. 4. Time-sequenced views of the surface of Pluto as seen from the Earth, for the 1954 and 1988 apparitions. The south pole appears as a dot for reference. Note how much the inclination has changed in 30 yr.

standard Russell–Merrill techniques or (more accurate) direct numerical simulation of the anticipated geometry for each event.

These events will serve to further improve the albedo model for Pluto as Charon selectively "maps out" different regions of Pluto's surface. Bumps and wiggles which repeat from transit event to transit event will serve to delineate precisely both the boundaries and albedos of individual Plutonian albedo features.

A more straightforward, if less stringent, test of the model can be made. When Pluto was discovered, any potential variability in its light curve went undetected. By extrapolation of our working model backward in time, after-the-fact predictions are possible, which can serve as a test of the utility of this model.

A synthetic light curve generated for the 1930 apparition predicts an amplitude of only 0.008 mag, clearly below the detection threshold of photographic photometry. The amplitude is predicted to have decreased further until 1943, when the planet was pole-on as seen from Earth and the light curve was flat. The light curve begins its monotonic growth from zero to a maximum of 0.291 mag sometime around the 1981 apparition. Figure 5 shows the theoretical envelope within which Pluto's brightness may be found for the years 1920–1990. To first order, any error in the value adopted for j_0 in Eq. (3) manifests itself as a shift in spot centers *equatorward* by a like amount, and delays this timeline by approximately one year per 2°.2.

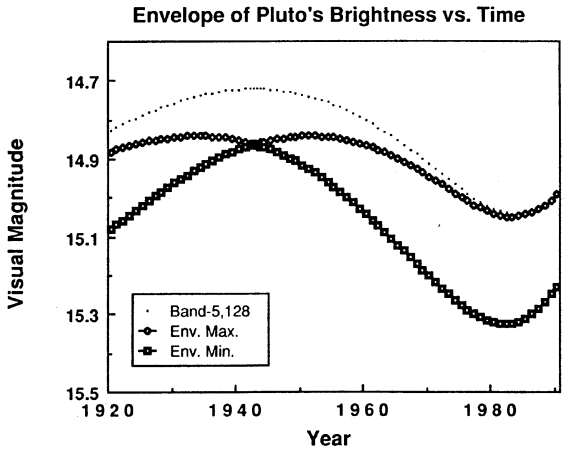

FIG. 5. Envelope of maximum and minimum light for 1920–1990. According to the adopted working model, Pluto's brightness can be expected always to be bounded by the two lower curves; the dashed curve represents the brightness modulation (orbital light curve) due to the bright polar caps.

Due to the synchroneity of all rotations in the Pluto–Charon system, Charon may be used to probe only those regions visible at rotational phase 0.25; the opposite hemisphere is never occulted by the satellite. More detailed mapping of the anti-Charon hemisphere of Pluto must await some future technique such as interferometric image reconstruction. The *Hubble Space Telescope* Faint Object Camera, with its anticipated resolution of 0.0072 arcsec/pixel (Paresce 1985), marginally will be able to confirm albedo spots, but can do nothing to further constrain their geometry. The angle subtended by Pluto's diameter is just over 5 pixels for this instrument.

The blurry picture of Pluto derived from spot modeling, along with certain refinements afforded by analysis of the mutual-event photometry, is yielding what is likely to be the clearest "image" of the Pluto–Charon system available for quite some time.

Thanks to my advisors, Drs. Douglas S. Hall, Robert H. Hardie, and Joel A. Eaton, for giving me the freedom and trust to "do what I thought was best" in this project. I am indebted to David Tholen and Richard Binzel for providing me with their data in advance of publication; they have since become valued friends and colleagues. My deepest heartfelt gratitude goes to Clint H. Poe and Carol J. Walsh. The many suggestions and insights they offered are appreciated almost as much as their friendship. This work was partially supported by NSF grant AST-8114594 and NASA grants NGT-50048 and NSG-7114.

APPENDIX: DERIVATION OF THE Δm RELATION

The total brightness observed at any rotational phase is given by the sum of contributions from Pluto and Charon,

$$l_{\rm obs} = l_{\rm C} + l_{\rm P} \tag{A1}$$

$$= A_{\rm C}\alpha_{\rm C} + A_{\rm P}\alpha_{\rm u} - A_{\rm s}\alpha_{\rm u} + A_{\rm s}\alpha_{\rm s}\,, \tag{A2}$$

where the subscripts C, P, s, and u refer to Charon, Pluto, spotted and unspotted, respectively. α represents the geometric albedo, and A the sum of all elements after projection and limb-darkening effects are individually taken into account.

These terms can be grouped into constant and time-varying quantities,

$$l_{\rm obs} = (A_{\rm C}\alpha_{\rm C} + A_{\rm P}\alpha_{\rm u}) - (A_{\rm s}\alpha_{\rm u} + A_{\rm s}\alpha_{\rm s})\,. \tag{A3}$$

We now define a reference brightness l_0 such that magnitude 0.000 corresponds to the combined brightness of the Pluto + Charon sum. Dividing through by l_0,

$$\frac{l}{l_0} = 1 - \frac{(A_{\rm s}\alpha_{\rm u} - A_{\rm s}\alpha_{\rm s})}{A_{\rm C}\alpha_{\rm u} + A_{\rm P}\alpha_{\rm u}}\,. \tag{A4}$$

We now assume that Charon's total area may be expressed as a fraction f of Pluto's total area:

$$A_{\rm C} = fA_{\rm P}\,. \tag{A5}$$

Substituting this convenience into Eq. (A4) yields

$$\frac{l}{l_0} = 1 - \frac{(A_{\rm s}\alpha_{\rm u} - A_{\rm s}\alpha_{\rm s})}{A_{\rm P}\alpha_{\rm u}(1+f)}\,. \tag{A6}$$

Factoring out $A_{\rm s}$ from the numerator of the last term, and dividing both numerator and denominator by $\alpha_{\rm u}$, yields

$$\frac{l}{l_0} = 1 - \frac{[A_{\rm s}(1 - \alpha_{\rm s}/\alpha_{\rm u})]}{A_{\rm P}(1+f)}\,. \tag{A7}$$

Now define the constant, albedo-dependent term of Eq. (A7) as ALBFAC, the so-called albedo factor. Further, we define the entirety of Eq. (A7) as the FORTRAN variable name BRITE. Expressed in magnitude units, we have our final form of the Δm equation,

$$\left.\begin{aligned} \Delta m &= -2.5\log(\text{BRITE}) \\ \text{BRITE} &= 1 - \frac{A_{\rm s}\times\text{ALBFAC}}{A_{\rm P}(1+f)} \\ \text{ALBFAC} &= (1 - \alpha_{\rm s}/\alpha_{\rm u}) \end{aligned}\right\}. \tag{A8}$$

Under the assumption of linear limb darkening, the finite-element approximation to $A_{\rm s}$ is given by

$$A_{\rm s} = \sum_i a_i(\hat{\mathbf{n}}_i\cdot\hat{\oplus})[1 - x + x(\hat{\mathbf{n}}_i\cdot\hat{\oplus})]\,, \tag{A9}$$

where a_i is the unprojected area of the ith element, $\hat{\mathbf{n}}_i$ is the normal of its center, $\hat{\oplus}$ represents the unit vector toward Earth, and the quantity x is the linear limb-darkening coefficient. The summation on i is taken over all spotted elements.

Note Added in Proof: Recent evidence, both observational (Sykes *et al.* 1987; Science **237**, 1336) and theoretical (Trafton *et al.* 1987; Icarus, in press) supports the plausibility of bright polar caps on Pluto. Although the Sykes *et al.* explanation for the *IRAS* observations of Pluto invokes polar caps of equal size, their total projected area is comparable to that of the two caps proposed in this paper. Further, the decrease in equivalent width of the 7200 Å CH_4 absorption between 1983 and 1987 (Fink and DiSanti 1988; Astron. J. **95**, 229) is consistent with the polar cap scenario. Photoelectric observations planned for the 1988 apparition of Pluto should provide the most direct evidence as to the existence and extent of the caps.

REFERENCES

Allen, C. W. (1973). *Astrophysical Quantities*, third ed. (Athlone, London), p. 142.

Andersson, L. E. (1974). Ph.D. thesis, Indiana University, Bloomington, IN.

Andersson, L. E., and Fix, J. D. (1973). Icarus **20**, 279.

Bevington, P. R. (1969). *Data Reduction and Error Analysis for the Physical Sciences* (McGraw–Hill, New York), p. 187.

Binzel, R. P., *et al.* (1985). Science **228**, 1193.

Binzel, R. P., and Mulholland, D. J. (1982). Astron. J. **88**, 222.

Binzel, R. P., and Mulholland, D. J. (1983). Astron. J. **89**, 1759.

Davies, M. E., *et al.* (1980). Celest. Mech. **22**, 205.

Eaton, J. A., and Hall, D. S. (1979). Astrophys. J. **86**, 442.

Hardie, R. H. (1965). Astron. J. **70**, 140.

Hardie, R. H. (1982). Personal communication.

Harrington, R. S., and Christy, J. W. (1981). Astron. J. **86**, 442.

Kiladze, R. I. (1967). Solar System Res. **1**, 173.

Lacis, A. A., and Fix, J. D. (1972). Astrophys. J. **174**, 449.

Lane, W. A., Neff, J. S., Andersson, L. E., and Fix, J. D. (1976). Publ. Astron. Soc. Pac. **88**, 77.

Marcialis, R. L. (1983). Master's thesis, Vanderbilt University, Nashville, TN. See AIP document no. PAPS ANJOA-95-941 for 91 pages of "A Two Spot Model for the Surface of Pluto". Order by PAPS number and journal reference from American Institute of Physics, Physics Auxiliary Publication Service, 335 East 45th Street, New York, NY 10017. The price is $1.50 for each microfiche (98 pages) or $5.00 for photocopies of up to 30 pages, and $0.15 for each additional page over 30 pages. Airmail additional. Make checks payable to the American Institute of Physics.

Marcialis, R. L. (1984). Bull. Am. Astron. Soc. **16**, 651.

Marcialis, R. L., Rieke, G. H., and Lebofsky, L. A. (1987). Science **237**, 1349.

Neff, J. S., Lane, W. A., and Fix, J. D. (1974). Publ. Astron. Soc. Pac. **86**, 225.

Paresce, F. (1985). *Faint Object Camera Instrument Handbook* (Space Telescope Science Institute, Baltimore, MD), p. 4.

Poe, C. H. (1983). Master's thesis, Vanderbilt University, Nashville, TN.

Renschen, C. P. (1977). Astron. Nachr. **298**, 179.

Russell, H. N. (1906). Astrophys. J. **24**, 1.

Taylor, R. C. (1979). In *Asteroids*, edited by T. Gehrels (University of Arizona, Tucson), p. 480.

Tedesco, E. F., and Tholen, D. J. (1980). Bull. Am. Astron. Soc. **12**, 729.

Tholen, D. J., and Tedesco, E. F. (1983). Bull. Am. Astron. Soc. **15**, 859.

Torres, C. A. O., and Ferraz-Mello, S. (1973). Astron. Astrophys. **27**, 231.

Vogt, S. S. (1975). Astrophys. J. **199**, 418.

Vogt, S. S. (1980). Astrophys. J. **240**, 567.

Walker, M. F., and Hardie, R. H. (1955). Publ. Astron. Soc. Pac. **67**, 224.